

Probing of the transverse momentum dependent parton distributions in nuclei

Yu. T. Kiselev

Institute for Theoretical and Experimental Physics

B.Chermushkinskaya 25, Moscow 117218, Russia

E-mail: yurikis@itep.ru

Analysis of data aimed at the determination of the mean transverse momentum squared, $\langle Pt^2 \rangle$, of pions, kaons, antikaons, proton, and antiprotons produced in cumulative reactions reveals new aspects of the nuclear structure at small-distance scales. The extracted X-dependence of $\langle Pt^2 \rangle$ exhibits two remarkable features. First, the values of the mean transverse momentum squared in the region of $X > 1$ significantly exceed those observed in the region of $X < 1$. Second, the values of $\langle Pt^2 \rangle$ are different for various types of hadrons. Studying of transverse momentum dependent distribution provides unique access to the orbital motion of partons inside nuclei.

*XXI International Baldin Seminar on High Energy Physics Problems
September 10-15, 2012
JINR, Dubna, Russia*

Understanding the internal structure of hadrons and nuclei on the basis of the fundamental theory of strong interactions, Quantum Chromodynamics (QCD), is one of the main goals of strong interaction physics. Therefore, a common goal of both particle and nuclear physics is to investigate the structure of the nucleon and nucleus in terms of their fundamental constituents. While impressive progress has been made in studying of the nucleon structure much less is known about the QCD structure of nuclei. Nuclei are stable systems, made up of quarks and gluons bound together by the strong force. However, the quarks and gluons are hidden and nuclei seem to be composed of nucleons bound together by the meson exchange. The quark-gluon structure of nuclei is an almost unexplored part of modern strong interaction physics.

The usage of lepton deep inelastic scattering (DIS) provides a power tool for determining the structure of nucleons in terms of quarks and gluons. Their behavior inside the nucleon is described by parton distribution functions (PDFs). Historically PDFs depended only on the fractional quark momentum longitudinal to the nucleon direction of motion, X , and on the scale at which the distributions were probed, Q^2 , while transverse degree of freedom were neglected. However, these degrees of freedom are not *a priori* negligible and are needed for a complete description of the nucleon. The concept of Generalized Parton Distributions (GPDs) was developed as a modern tool to deliver a detailed description of the *of-forward* microscopic structure of hadrons in terms of their elementary constituents [1], [2]. GPDs contain the extensive information on the spatial hadron structure which can be studied in deeply virtual Compton scattering (DVCS) as well as in deeply virtual light meson leptonproduction (DVMP) on the basis of the handbag approach [3], [4]. The new t -channel variables allow one to pin down *in principle* the dependence of the parton distributions on spatial degree of freedom through Fourier transforms of GPDs.

One of the most surprising results of the lepton scattering experiments is unexpectedly small fraction, about a quarter, of the proton's spin that is due to the contribution from quarks and antiquarks. New concept of Transverse Momentum Dependence (TMD) distributions and fragmentation functions [5], [6], which go beyond the collinear approximation can provide the information about the spin of the nucleon. Since the total spin of the nucleon consists of the orbital momentum and intrinsic contributions of the u and d quarks respectively, the studying of TMDs provide a novel way to measure the fraction of the nucleon spin carried by the quark orbital angular momentum, a subject of great current interest. These TMD distributions together with GPDs, for the first time, provide a framework for obtaining the information on multi-dimensional structure of the nucleon (see [7] for recent review).

The normal nuclear density of $0.16\text{--}0.17$ nucleon/ fm^3 corresponds to the average inter-nucleon (center-to-center) distance of $1.8\text{--}2$ fm. Comparing this value with the electromagnetic radius of a proton $r_{em} = 0.83$ fm shows that nucleons are tightly packed inside nuclei and almost overlap. Owing to quantum fluctuations of nuclear density, two or more nucleons can get even closer, forming dense cold compact baryonic configurations (CBCs). Current estimates of CBC size vary from 0.65 to 1 fm [8, 9, 10], which corresponds to a density about four- to eightfold the normal nuclear density.

These values are comparable with those expected in the cores of neutron stars. In conventional nucleon-meson nuclear physics, CBCs are described as collections of closely packed nucleons usually referred to as short-range correlations (SRCs) of nucleons [11]. However, one can expect that the densities of CBCs are high enough to modify the structure of underlying nucleon constituents. At short inter-nucleon distances, nucleons can lose their identities and form multiquark configurations [10, 12, 13] or multinucleon quark clusters [14]. The existence of locally dense objects in nuclei provides the possibility to extend the study of hadron production to the region of $X > 1$ in order to obtain information on the internal structure of CBCs. The uncertainty principle requires that such hadrons could arise from fluctuations of dense CBCs consisting of either a few closely packed nucleons with a high relative momentum [11] or quark constituents of a multiquark configuration carrying a light cone momentum fraction greater than that of a single nucleon [10].

Measurements of ratios of inclusive DIS cross section on different nuclei to that on deuteron in the range of the Bjorken scaling variable $1 < X_B < 2$ and moderate $1.4 < Q^2 < 2.6$ GeV² was carried out in JLab [15,16]. The combine analysis of these data and new high-precision experimental data on the EMC effect in light nuclei obtained at JLab [17] reveals a clear linear correlation between the strength of the EMC effect, defined as the slope of the cross-section ratios in the range $0.3 < X_B < 0.7$, and the nuclear scaling plateaus at $X_B > 1$ [18]. These results are consistent with the idea that both effects scale with the local nuclear environment. One can expect that the properties of multiquark configurations differ from those of nucleonic SRCs. Remind, that the discovery of the EMC effect 30 years ago [19] clearly demonstrated that even in the region of $X_B < 1$ the inelastic scattering cross section for scattering from bound nucleons differs from that of free nucleons. As was pointed in [8] in DIS experiments at $1.5 < Q^2 < 4$ GeV² SRCs between nucleons can be resolved, while at higher Q^2 the exploration of the quark-gluon structure of high density nuclear configuration becomes possible. Thus, the investigation of the region $X_B > 1$ can help to elucidate the fundamental nature of nuclear matter.

Studying cumulative reactions provides complementary information on localized dense objects inside nuclei. Cumulative hadron production can be the key to understanding the process of hadron creation in the fragmentation region of a nucleus beyond the kinematical limits of the production of these hadrons in the collisions of elementary projectiles with isolated nucleons. In 1980–1990s cumulative hadron production was intensively investigated in many experiments using a variety of beam particles and energies. Proton-induced production of high-momentum cumulative protons, pions, kaons, antikaons, and antiprotons [9, 20] has been studied at ITEP up to the value of $X \approx 3.5$, where X is a variable which differs from the Bjorken X_B by the account for mass corrections. The value of the longitudinal variable X can be obtained from Eq. (1), expressing conservation of the energy-momentum, strangeness, and baryonic number in the reaction $I+II \rightarrow 1+\dots$

$$\left(P_I + X \frac{P_{II}}{A} - P_1\right)^2 \geq \left(M_I + X \frac{M_{II}}{A} + m_2\right)^2 \quad (1)$$

where P_I , P_{II} , P_1 are 4-momenta of projectile particle, target nucleon and detected hadron, respectively; A stands for target atomic mass number; $m_2=0$ for pions, $m_2=m_K$ for K^- -mesons and so on. With the condition of minimal missing mass in the reaction, corresponding to the equality of the left- and right-hand sides of Eq. (1), one find the result that

$$X = \frac{(P_I \cdot P_1) + M_I \cdot m_2 + \frac{m_2^2 - m_1^2}{2}}{(P_I \cdot P_{II}) - M_I \cdot M_{II} - (P_{II} \cdot P_1) - M_{II} \cdot m_2} \quad (2)$$

The value $X = 1$ corresponds to the kinematical limit of hadron creation on a nucleon at rest, while in the cumulative region $X > 1$.

The example of per-nucleon invariant cross sections of cumulative hadron production by 10-GeV protons on copper target as functions of X is shown in Fig.1.

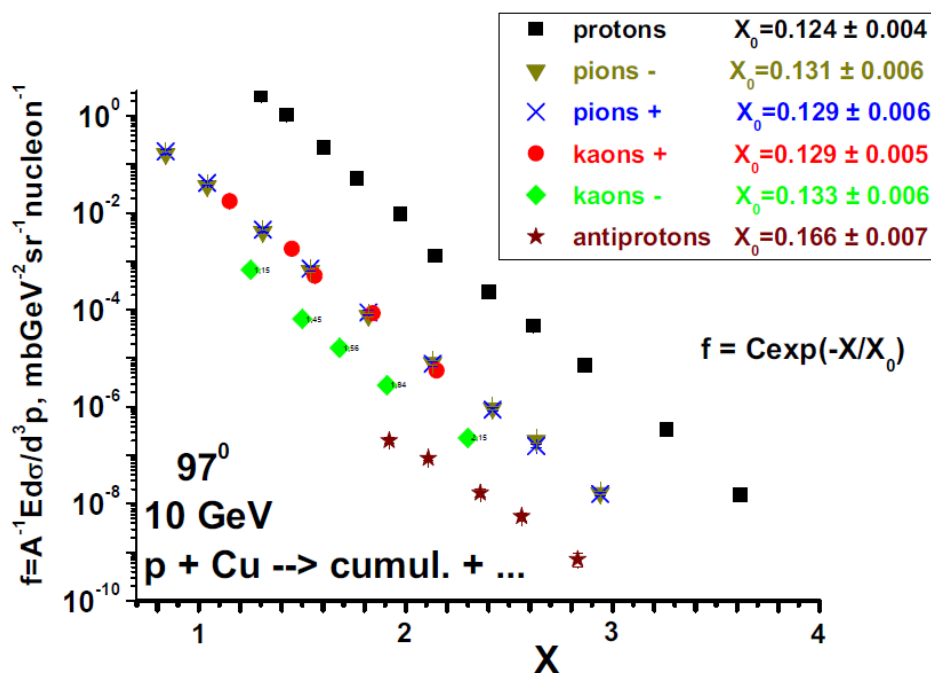


Fig.1. (Color online) Invariant cross sections for the production of cumulative protons (squares), π^+ -mesons (crosses), K^+ -mesons (circles), K^- -mesons (diamonds), and antiprotons (stars) as functions of X . The errors bars are less than size of symbols. Data are from Ref. [9, 20].

The observed change of cross sections within the measured range of X is ten orders of magnitude. However, the spectra have universal form. The measure of proximity of spectra in case of exponential fitting to the experimental data by the function $f=Cexp(-X/X_0)$ is a scatter of inverse slope parameters X_0 . The magnitudes X_0 , shown in the legend, are equal within $\sim 5\%$ accuracy for all types of cumulative particles except

for antiprotons for which the mass corrections are maximal. The remarkable feature of the data is enhanced strangeness production. The cross section ratio for K^+ -mesons and π^+ -mesons is close to unity for middle and heavy nuclei in contrast to that observed in proton-proton collisions. The very interesting facet of cumulative hadron production is that the cross section ratio for ‘sea’ K^- -mesons and ‘valence’ π^- -mesons does not depend of X while this ratio measured in proton-proton reactions decreases rapidly when $X \rightarrow 1$. These features of the cumulative process has no explanation in any model where nuclei are made of nucleons and evidence for the properties of the source of cumulative particles differ from those of nucleonic SRCs.

Knowing invariant cross sections $f(X)$ measured at different production angles allows one to draw a conclusion about their transverse momentum dependence. Eq.3 determines the probability of hadron production with given P_t^2 relative to that with $P_t^2=0$.

$$\Phi = \frac{f(X, P_t^2)}{f(X, P_t^2 = 0)} \quad (3)$$

The transverse momentum dependence of the function Φ for the π^+ -mesons and K^+ -mesons at different X is presented in Fig.2. Along with the cross sections measured in our experiments [9,20] at laboratory angles 97° and 119° we also use the data on cumulative hadron production obtained at 90° , 120° and 180° in very similar kinematical conditions [21].

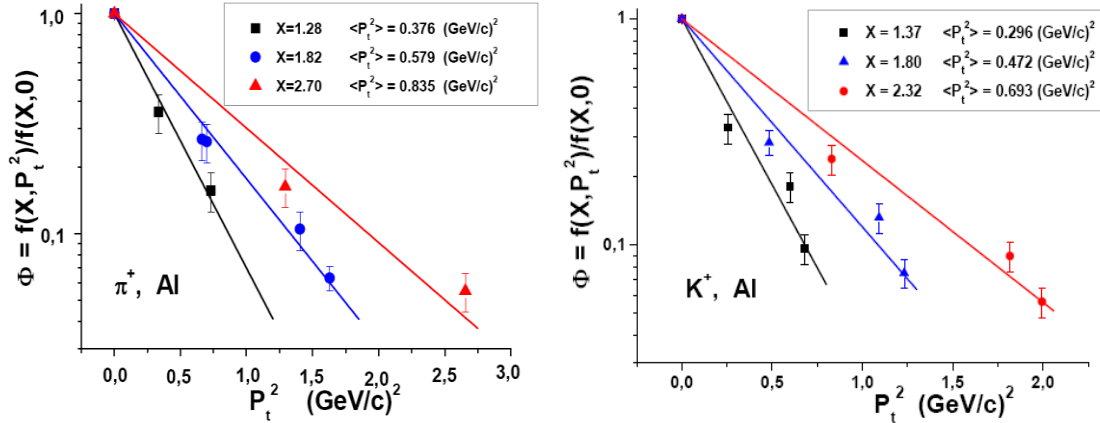


Fig.2. (Color online) Cross section ratio measured on Al target as a function of transverse momentum squared for π^+ -mesons (left) and K^+ -mesons (right) at different X . Data are from Ref.[9, 20, 21].

The broadening of the $\Phi(P_t^2)$ distribution with increasing of X is observed for all types of cumulative hadrons. To a first approximation the function Φ was parameterized as $\Phi(P_t^2)=\exp(-\gamma P_t^2)$, and the values of mean transverse momentum squared for different magnitudes of X were calculated using Eq.4.

$$\langle P_t^2 \rangle = \frac{\int_0^{\infty} P_t^2 \exp(-\gamma P_t^2) dP_t^2}{\int_0^{\infty} \exp(-\gamma P_t^2) dP_t^2} = \frac{1}{\gamma} \quad (4)$$

These values, indicated in the legends of Fig.2, demonstrate the sizable increase of $\langle P_t^2 \rangle$ with X. However, simple exponential approximation of $\Phi(P_t^2)$ yields typical values of $\chi^2/\text{ndf} \sim 2$. More detail analysis of data shows that $\Phi(P_t^2)$ -dependence has two component structure and becomes less steep at the region of high transverse momenta (Fig.3).

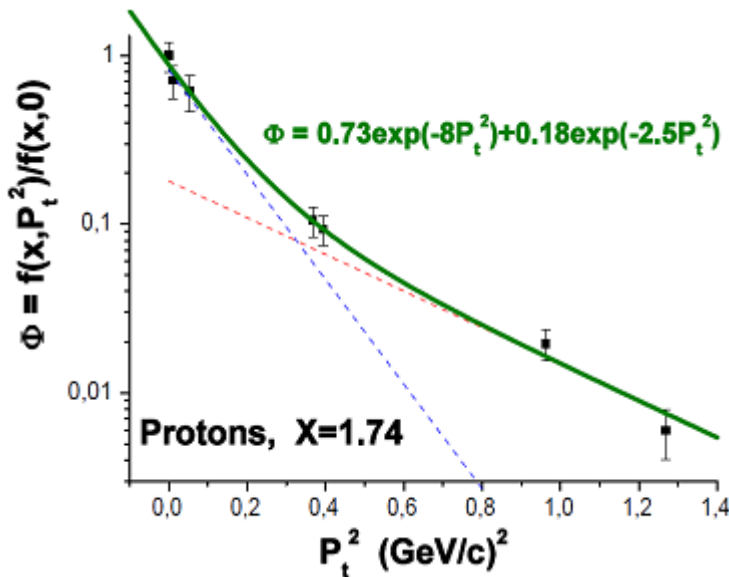


Fig.3. (Color online) Cross section ratio for protons production on Al target as a function of transverse momentum squared. Dashed lines represent contributions of two components. Data are from Ref. [9, 20, 21].

To analyze the high momentum component of the $\Phi(P_t^2)$ -distribution in more detail, in the subsequent analysis we use only the data of our experiment obtained at 97^0 and 119^0 in the laboratory system. The cross section ratios (Eq.3) measured in one experiment can be determined more precisely than the absolute values of cross sections, as the detector-dependent errors, many of the correction factors, and most of the absolute normalization uncertainty cancels out in the ratios. Besides, it permits us to include into analysis K^- - mesons and antiprotons in spite of the data on the production of these particles at small transverse momentum are not available. Since data do not reveal a significant target mass dependence we evaluated the values of $\langle P_t^2 \rangle$ using Eq.4 and then averaged them over A (A=Be, Al, Cu, Ta). The result is presented in Fig.4.

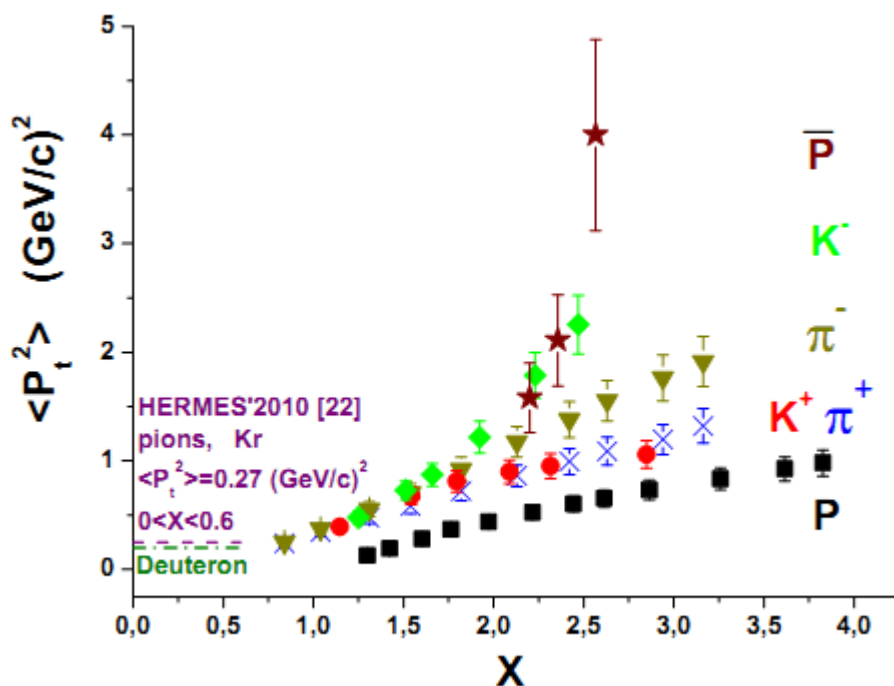


Fig.4. (Color online) Mean transverse momentum squared versus X for protons (squares), π^+ -mesons (crosses), K^+ -mesons (circles), K^- -mesons (diamonds), and antiprotons (stars). Data are from Ref. [9, 20, 22].

A measurement of the hadron transverse momentum broadening $\Delta\langle P_t^2 \rangle = \langle P_t^2 \rangle_A^h - \langle P_t^2 \rangle_D^h$ has been performed by the HERMES collaboration using the set of nuclear targets and a deuteron target [22]. In the vicinity of $X=1$ our results for pions agree well with those obtained in [22]. In the region of $X>1$ values of the mean transverse momentum squared strongly increase with X and sizably exceed those observed in the region of $X<1$. The remarkable feature of the data shown in Fig.4 is that the relation between $\langle P_t^2 \rangle$ and X depends on the quark content of cumulative particles. Most strong effect is observed for ‘sea’ K^- -mesons and antiprotons. Significant difference between the values of the mean transverse momentum squared for deuterons (nucleons) and CBCs evidences in favor of the quark structure of locally dense objects in nuclei. Note that X-dependence of $\langle P_t^2 \rangle$ for negative pions and protons was reasonably described in Quark Gluon String Model (QGSM) based on $1/N$ expansion in QCD [23]. Therefore, the extension of QGSM to the description of strange mesons and antiprotons is highly desirable.

It is commonly believed that TMD parton distributions can be extracted, albeit in a model-dependent way, from measurements of the nuclear broadening of the transverse momentum distribution for hadrons in the region of $X<1$. Similarly, the data presented in Fig.4 can provide the information about TMD parton distributions inside CBCs. The

observation of large values of $\langle P_T^2 \rangle$ in the region of $X > 1$ indicates a medium modification of TMD distributions inside locally dense objects existing in nuclei.

In conclusion, the study of Compact Baryon Configurations - objects of the nuclear structure at small-distance scales – offers the possibility to investigate the quark and gluon degrees of freedom in nuclei as well as the equation of state of a cold and dense matter. Besides, the high density of CBCs provides unique possibility to study QCD diagram in the unexplored range of low T and high baryonic potential μ_B .

References

1. Xiangdong Ji Phys. Rev. D 55 (1997) 7114; Phys. Rev. Lett. 78 (1997) 610.
2. A.V.Belitsky, A.V.Radushkin Physics Reports 418 (2005) 1.
3. S. V. Goloskokov arXiv: 1111.5407 [hep-ph].
4. G. R. Goldstein *et al.*, Phys. Rev. D 84, 034007 (2011).
5. P.J. Mulders and R.D. Tangerman, Nucl. Phys. B461 (1996) 197.
6. A. Bacchetta *et al.*, JHEP 02 (2007) 093; arXiv: hep-ph/0611265
7. H. Avakian *et al.*, arXiv: 1202.1910 [hep-ex].
8. M. M. Sargsian *et al.*, J. Phys. G 29, R1 (2003).
9. S.V.Boyarinov *et al.*, Yad. Fiz. 50, 1605 (1989) [Sov. J. Nucl. Phys. 50, 996 (1989)].
10. A. V. Efremov *et al.*, Yad. Fiz. 57, 932 (1994) [Phys. Atom. Nucl. 57, 874 (1994)].
11. L. L. Frankfurt and M. I. Strikman, Phys. Rep. 76, 215 (1991); 160, 235 (1998).
12. G. Berlhad, A. Dar, and G. Eilam, Phys. Rev. D 22, 1547 (1980).
13. M. A. Braun, V. V. Vechernin, Nucl. Phys. B 427, 614 (1994).
14. H. J. Pirner and J. P. Vary, Nucl. Phys. A 358, 413c (1981).
15. K. Egiyan *et al.*, Phys. Rev. C 68, 014313 (2003); Phys. Rev. Lett. 96, 082501 (2006).
16. N. Fomin, Ph.D. thesis, University of Virginia (2007), arXiv:0812.2144 [nucl-ex].

17. J. Seely *et al.*, Phys. Rev. Lett. 103, 202301 (2009).
18. L.B. Weinstein, E. Piasetzky, D. W. Higinbotham, J. Gomez, O. Hen, and R. Shneur, Phys. Rev. Lett. 106, 052301 (2011).
19. J. Aubert *et al.*, Phys. Lett. B 123, 275 (1983).
20. S. V. Boyarinov *et al.*, Yad. Fiz. 57, 1452 (1994) [Phys. Atom. Nucl. 57, 1379 (1994)]; Yad. Fiz. 54, 119 (1991) [Sov. J. Nucl. Phys. 54, 71 (1991)]; Yad. Fiz. 56, 125 (1993) [Phys. Atom. Nucl. 56, 72 (1993)].
21. A. M. Baldin *et al.*, Preprint JINR E1-82-472 (1982); Preprint JINR E1-83-432 (1983).
22. A. Airapetian *et al.*, Phys. Lett. B684, 114 (2010).
23. A. B. Kaidalov *et al.*, Proc.of IX Int. Seminar on High Energy Physic Problems, Vol.1, p.271, Dubna 1988.